

Photon-pair blockade in a Josephson-photonics circuit with two nondegenerate microwave resonators

Sheng-li Ma¹, Ji-kun Xie¹, Ya-long Ren¹, Xin-ke Li^{2,*} and Fu-li Li^{1,*}

¹ MOE Key Laboratory for Non-equilibrium Synthesis and Modulation of Condensed Matter, Shaanxi Province Key Laboratory of Quantum Information and Quantum Optoelectronic Devices, School of Physics, Xi'an Jiaotong University, Xi'an 710049, China

² School of Mathematics, Physics and Optoelectronic Engineering, Hubei University of Automotive Technology, Shiyan 442002, China

E-mail: 20210064@huat.edu.cn and flli@mail.xjtu.edu.cn

Abstract. We propose to generate photon-pair blockade in a Josephson-photonics circuit that consists of a dc voltage-biased Josephson junction in series with a superconducting charge qubit and two nondegenerate microwave resonators. The two-level charge qubit is utilized to create anticorrelations of the charge transport; that is, the simultaneous Cooper pair tunneling events are inhibited. When the Josephson frequency matches the sum of resonance frequencies of the charge qubit and the two resonators, we demonstrate that the two resonators can release their energies in the form of antibunched pairs of two strongly correlated photons. The present work provides a practical way for producing a bright microwave source of antibunched photon pairs, with potential applications ranging from spectroscopy and metrology to quantum information processing.

30 March 2022

1. Introduction

Solid-state superconducting circuit studies the interaction between artificial atoms and quantized electromagnetic fields in the microwave frequency domain [1]. This architecture has emerged as one of the leading platforms for realizing quantum computation and simulation [2, 3]. Commonly, superconducting qubits are used for encoding quantum information, with superconducting resonators acting as data buses. However, the efficient generation, manipulation, and transmission of nontrivial quantum states in a linear resonator are also crucial to different kinds of quantum information tasks [4]. The quantum states of a harmonic oscillator are extraordinarily rich, but are hard to access due to the infinitely equally spaced energy levels. This difficulty can be overcome by interposing a nonlinear artificial atom, and various quantum states in a

resonator can be synthesized via the deliberate use of classical control signals, such as Fock state [5] and Schrödinger cat state [6].

In recent years, the Josephson-photonics circuit of a dc voltage-biased Josephson junction in series with a microwave resonator has emerged as an alternative tool for efficient on-chip generation of coherent microwave photons [7–16]. It relies on the exceptionally strong nonlinearity of light-charge interaction, and eliminates the need for any microwave drives [17–21]. The Josephson junction acts as a highly nonlinear driving element; that is, the inelastic Cooper pair tunneling across a junction can convert different numbers of photons from an easily controlled bias voltage source into a microwave cavity [22, 23]. By modulating the charge tunneling effect via a specifically tailored electromagnetic environment, the nonclassical microwave light can be generated [24–29]. The resulting quantum electrodynamics of this simple circuit has been demonstrated to realize Josephson junction lasers [30–32], single-photon sources [33–36], multi-photon sources [37–39], and near quantum-limited amplifiers [40].

In parallel, a significant development in this field is to connect Josephson junctions with multiple resonators for various quantum technological applications, such as the implementations of entangled quantum microwaves [41] and microwave single-photon detectors [42]. While the simplest case is one voltage-biased junction in series with two cavities of incommensurate frequencies. When the bias voltage is tuned to match the energy required to simultaneously produce one photon in each cavity for a single Cooper pair traversing the circuit, the system can be effectively reduced as a nondegenerate parametric amplifier [43–45]. It allows the continuous emission of correlated photon pairs. Recent experiments have observed the amplitude squeezing [46] and entanglement [47] of these output microwave beams. Especially, when the cavities possess the impedance of 4.1 k Ω , there is no matrix element for a transition between the one and two photon states [23, 35]. So, the two cavities can be regarded as two-level systems, leading to an antibunched photon-pair source [43]. However, the fabrication of coplanar waveguide resonators with such high impedances is highly challenging as the standard cavity designs only yields characteristic impedances of the order of 100 Ω .

To go beyond this limitation, we propose a more practical way to realize photon-pair blockade by regulating the anticorrelated behavior of the charge transport via a two-level charge qubit. In our scheme, we study the Josephson-photonics device of a voltage-biased Josephson junction in series with a charge qubit and two nondegenerate microwave resonators. The nonlinear qubit-resonator coupling can be sculpted via the phase difference across the junction. For each tunneling Cooper pair, the suitably set bias voltage enables the excitation of charge qubit and the creation of one photon in each resonator concurrently. Since the charge qubit is an ideal anharmonic element with two quantum energy levels, the anticorrelations of the tunneling Cooper pairs can be created, preventing the simultaneous tunnel events. Combined with the dissipation, we show that the two resonators can release their energies in the form of antibunched photon pairs in a controllable manner. Compared with the previous work [43], the present one constitutes a significant step forward; that is, the photon-pair source can be

achieved with the standard coplanar waveguide resonator designs, eliminating the need for ultrahigh cavity impedance that is not accessible in current experiment. Our work offers an appealing method for generating a bright nonclassical source of antibunched pairs of two strongly correlated photons, required at the core of quantum computing and quantum communication protocols [48–51].

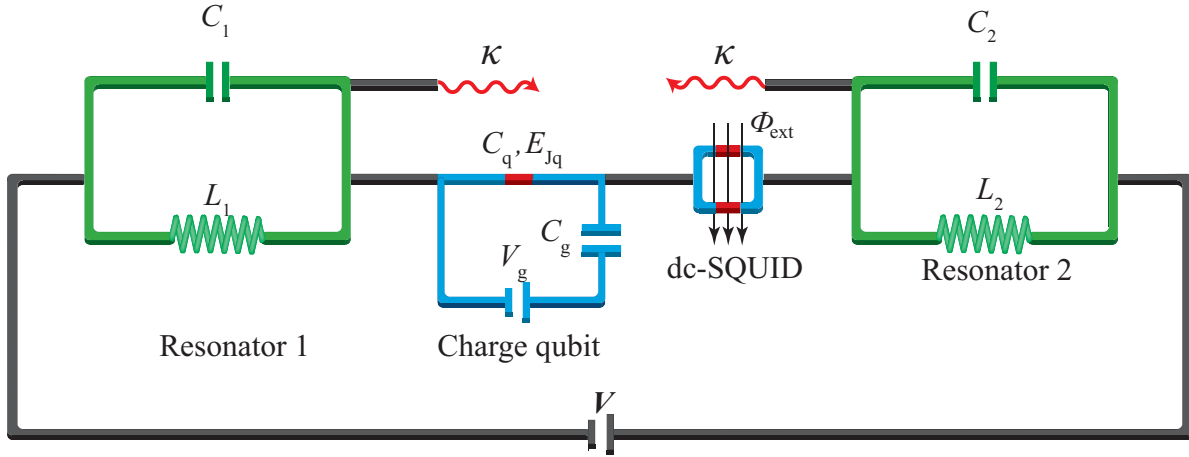


Figure 1. Schematic diagram of the proposed experimental setup that consists of a dc-SQUID coupled to a charge qubit and two nondegenerate LC resonators. A dc bias voltage V is applied across all the elements, and a flow of Cooper pairs across the circuit can pump both the qubit and the two LC resonators. In addition, each resonator is coupled to a transmission line with the coupling strength κ , which is used for collecting the emitted photons.

2. Model

As shown in Figure 1, we investigate the Josephson-photonics circuit of a voltage-biased dc superconducting quantum interference device (dc-SQUID) in series with a charge qubit and two nondegenerate LC resonators. We focus on the situation that the bias voltage V is smaller than the gap voltage, and no quasi-particle excitation can be produced in the superconducting electrodes. So, the quantum transport of Cooper pairs through the circuit will supply energies to both the charge qubit and the two LC resonators. The model Hamiltonian describing the entire setup takes the form (see Appendix)

$$\begin{aligned}
 H_T = & E_c(n_q - n_g)^2 - E_{Jq} \cos \phi_q + \sum_{j=1,2} \left[\frac{q_j^2}{2C_j} + \left(\frac{\hbar}{2e} \right)^2 \frac{\phi_j^2}{2L_j} \right] \\
 & - E_J \cos \phi_J - 2en_J(V - V_q - V_{R1} - V_{R2}).
 \end{aligned} \tag{1}$$

The first two terms denote the part of charge qubit, the third term describes the part of two LC resonators, and the last two terms represent the part of dc-SQUID, where

$V_q = -\hbar\dot{\phi}_q/2e$ is the voltage drop at the qubit, and $V_{Rj} = -\hbar\dot{\phi}_j/2e$ is the voltage drop at the j -th resonator.

To exclude the Cooper pair number n_J , we perform a unitary transformation $U(t) = \exp[i(\omega_J t + \phi_q + \phi_1 + \phi_2)n_J]$ on the full Hamiltonian, where $\omega_J = 2eV/\hbar$ is the Josephson frequency. Then, we can obtain

$$\begin{aligned}\tilde{H}_T &= U^\dagger(t)H_T U(t) + i\hbar\frac{dU^\dagger(t)}{dt}U(t) \\ &= E_c(\tilde{n}_q - n_g)^2 - E_{Jq}\cos\eta_q + \sum_{j=1,2}\left[\frac{\tilde{q}_j^2}{2C_j} + \left(\frac{\hbar}{2e}\right)^2\frac{\phi_j^2}{2L_j}\right] \\ &\quad - E_J\cos(\omega_J t + \phi_q + \phi_1 + \phi_2),\end{aligned}\tag{2}$$

where $\tilde{n}_q = n_q + n_J$, $\tilde{q}_j = q_j + 2en_J$ are the transformed number and charge operators, arising from the charge fluctuations regard to the flow of Cooper pairs through the dc-SQUID. As described by the last term in \tilde{H}_T , the nonlinear coupling between the charge qubit and the two cavities is established via the phase difference across the junctions of dc-SQUID.

When the charge qubit is operated at the degeneracy point with $n_g = 1/2$, we can quantize the excitations in the two resonators and qubit, and the Hamiltonian of the whole circuit will yield (hereafter let $\hbar = 1$)

$$H = \frac{1}{2}\delta\sigma_z + \sum_{j=1,2}\omega_j a_j^\dagger a_j - E_J\cos[\omega_J t + \phi_q + \sum_{j=1,2}2\lambda_j(a_j^\dagger + a_j)].\tag{3}$$

Note that the charge qubit has been reduced as a two-level system containing an excited state $|e\rangle$ and a ground state $|g\rangle$ under the basis of charge states [52–55], i.e., $\sigma_z = |e\rangle\langle e| - |g\rangle\langle g|$ is the Pauli matrix, and $\delta = E_{Jq}$ is the energy splitting. a_j^\dagger (a_j) is the photon creation (annihilation) operator of the j th resonator ($[a_j, a_j^\dagger] = 1$), and $\omega_j = 1/\sqrt{L_j C_j}$ is the corresponding resonance frequency. The parameter $\lambda_j = \sqrt{\pi Z_j/R_K}$ quantifies the amplitude of the cavity's zero-point displacement, and characterizes the coupling between the oscillator and the tunnel junction ($Z_j = \sqrt{L_j/C_j}$ is the characteristic impedance, and $R_K = h/e^2$ is the resistance quantum).

3. Photon-pair blockade

3.1. Anticorrelations of the charge transport

In this section, we will illustrate the procedure for the realization of photon-pair blockade in the aforementioned two-mode superconducting circuit. The central idea is to create anticorrelations of the charge transport, which gives rise to the desired antibunching of the photon pairs leaking out of the two microwave resonators.

To this end, we start to derive the effective Hamiltonian of the system, which helps to uncover the mechanism of our scheme. In the interaction picture with respect to the

frame rotating $\exp(-iH_0t)$, where $H_0 = \frac{1}{2}\delta\sigma_z + \omega_1 a_1^\dagger a_1 + \omega_2 a_2^\dagger a_2$ is the free Hamiltonian, we can obtain

$$H_I = -\frac{E_J}{4} e^{i\omega_J t} (\sigma_+ e^{i\delta t} - \sigma_- e^{-i\delta t} - \sigma_z) D[\alpha_1(t)] \times D[\alpha_2(t)] + h.c., \quad (4)$$

where we have exploited the formula $e^{i\phi q} = (\sigma_+ - \sigma_- - \sigma_z)/2$, and $\sigma_+ = |e\rangle\langle g|$, $\sigma_- = |g\rangle\langle e|$ are the spin-ladder operators. In addition, $D[\alpha_j(t)]$ is the cavity displacement operator with the time-dependent amplitude $\alpha_j(t)$, which is defined in terms of the photon creation and annihilation operators as

$$D[\alpha_j(t)] = e^{[\alpha_j(t)a_j^\dagger - \alpha_j^*(t)a_j]}, \quad \alpha_j(t) = 2i\lambda_j e^{i\omega_j t}. \quad (5)$$

It is now clearly seen that the tunneling of Cooper pairs through a voltage-biased Josephson junction can not only displace the cavity fields, but also flip the qubit state. To formulate the desired coupling, we express $D[\alpha_j(t)]$ directly in the Fock-state basis [56]

$$D[\alpha_j(t)] = \sum_{n=0}^{\infty} \left(\sum_{l=0}^{\infty} \beta_n^{n+l}(\lambda_j) |n+l\rangle\langle n| e^{il\omega_j t} + \sum_{l'=1}^{\infty} \beta_n^{n+l'}(\lambda_j) |n\rangle\langle n+l'| e^{-il'\omega_j t} \right) \quad (6)$$

with

$$\beta_n^{n+l}(\lambda_j) = \sqrt{\frac{n!}{(n+l)!}} (2i\lambda_j)^l e^{-2\lambda_j^2} L_n^{(l)}(4\lambda_j^2). \quad (7)$$

Here $\beta_n^{n+l}(\lambda_j)$ is a generalized Frank-Condon factor that describes an l -photon transition rate, and $L_n^{(l)}(4\lambda_j^2)$ is a Laguerre polynomial.

To go a further step, we should tune the bias voltage V to meet the resonance condition $\omega_J = \delta + \omega_1 + \omega_2$, i.e., the energy provided by the voltage source upon the transfer of a Cooper pair matches the sum of the excitation energy of qubit and the photon energies of the two oscillators. In this case, we can retain the resonant terms, but discard those fast oscillating terms under the rotating-wave approximation provided that the condition $\delta, \omega_j, |\omega_1 - \omega_2| \gg \frac{E_J}{4} |\beta_n^{n+l}(\lambda_1) \beta_m^{m+l'}(\lambda_2)|$ is satisfied. Thus, with all the other possibilities strongly suppressed, the effective Hamiltonian is derived as

$$H_{eff} = \sum_{n,m=0}^{\infty} H_{nm} \quad (8)$$

with

$$H_{n,m} = g_{eff}^{n,m} |n, m, g\rangle\langle n+1, m+1, e| + h.c., \quad (9)$$

where $g_{eff}^{n,m} = \frac{E_J}{4} \beta_n^{n+1}(\lambda_1) \beta_m^{m+1}(\lambda_2)$ is the effective coupling strength, and $|n, m, g\rangle$ is the tensor product of $|n\rangle \otimes |m\rangle \otimes |g\rangle$.

The effective Hamiltonian H_{eff} elucidates the process of energy conversion of Josephson frequency to qubit excitation and photon production in the two resonators. Note that each subunit $H_{n,m}$ can induce a coherent quantum transition from the state $|n, m, g\rangle$ to $|n+1, m+1, e\rangle$; that is, each Cooper pair can tunnel to simultaneously populate the qubit and add one photon in each cavity. Since the charge qubit is a two-level system, its excitation will greatly inhibit the whole system's transitions to higher

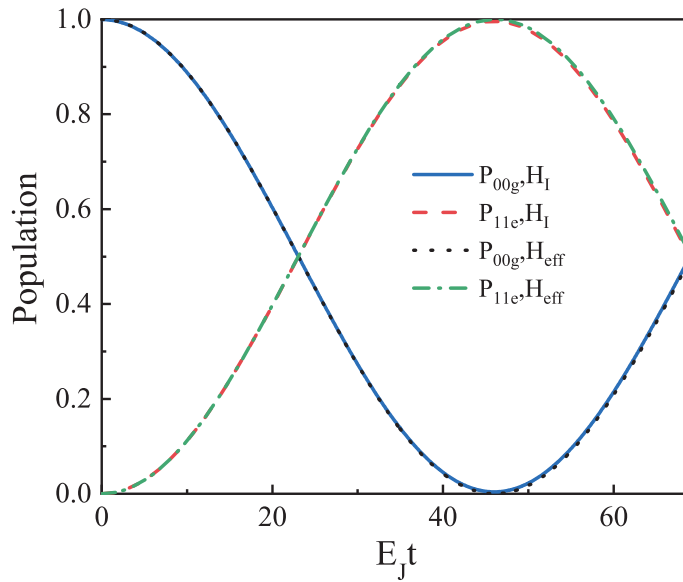


Figure 2. (Color online) Time evolution of the state populations P_{00g} and P_{11e} . The blue solid and red dashed curves are simulated with the original Hamiltonian H_I , while the black dotted and green dash-dotted curves are achieved with the effective Hamiltonian H_{eff} . The relevant parameters are chosen as $\omega_1/2\pi = 9$ GHz, $\omega_2/2\pi = 7$ GHz, $\delta/2\pi = 5$ GHz, $E_J/2\pi = 0.5$ GHz, and $\lambda_1 = \lambda_2 = 0.2$.

occupations. Thus, the anticorrelations of the charge transport are created: a former Cooper-pair tunneling event acts back onto the next one; that is, a second Cooper pair can not pass through the circuit until the flip of the qubit state. This is the key point to induce antibunching in the photon emission.

If the system is initially prepared in the ground state $|0, 0, g\rangle$, the Hamiltonian $H_{0,0}$ will dominate the dynamics, enabling a Rabi oscillation $|0, 0, g\rangle \longleftrightarrow |1, 1, e\rangle$. Obviously, the absorption of one photon in each cavity is accompanied with a excitation in the charge qubit. Since the charge qubit is treated as a two-level system, its excitation will inhibit further photon absorption, which is the mechanism involved in photon blockade [57, 58]. Consequently, the photon-pair blockade can be realized in this two-cavity system, which offers a source of antibunched pairs of two strongly correlated photons. It is also pointed out here that the charge qubit has finite nonlinearity in practice, and many other higher excited states exist. So, the excitation of these states is accompanied with the higher photon number excitations, which will degrade the photon blockade. However, the charge qubit is operated in the regime in which the charging energy E_c is much larger than the Josephson coupling energy E_{Jq} [52–55]. The third energy level has a eigenfrequency about $6E_c$, which is far greater than the transition frequency E_{Jq} of the lowest two energy levels. So, the higher-order qubit excitations are greatly inhibited, which has negligible effect on the photon blockade. Compared with the previous proposal [43], our scheme can be implemented with the standard coplanar waveguide resonator designs, greatly lowering the requirement for ultrahigh cavity impedance that is not accessible in current experiment.

To check the validity of the approximation, we now investigate the dynamics of the system by numerically solving the Schrödinger equation with both the full Hamiltonian H_I and the effective Hamiltonian H_{eff} . With the system initialized in the ground state $|0, 0, g\rangle$, the time evolution of populations P_{00g} in the state $|0, 0, g\rangle$ and P_{11e} in the state $|1, 1, e\rangle$ is shown in Figure 2. The perfect Rabi oscillations $|0, 0, g\rangle \longleftrightarrow |1, 1, e\rangle$ are observed with both of these two Hamiltonians H_I and H_{eff} , implying that our approximation is valid.

3.2. Antibunched photon pair emission

As a trigger of quantum emission of antibunched photon pairs, dissipation has to be taken into account. When the system-environment coupling is considered in the Born-Markov approximation, the time evolution of density matrix ρ of the whole system is now governed by the master equation

$$\frac{d\rho}{dt} = -i[H_{eff}, \rho] + \sum_{j=1,2} \frac{\kappa}{2} D[a_j]\rho + \frac{\gamma}{2} D[\sigma_-]\rho, \quad (10)$$

where $D[o]\rho = 2o\rho o^\dagger - o^\dagger o\rho - \rho o^\dagger o$ is the standard Lindblad operator for a given operator o , and κ (γ) denotes the energy damping rate of cavities (qubit). In the presence of dissipation, a pair of two strongly correlated photons will be transferred outside of the two cavities for each tunneling Cooper pair. We now detail the underlying principle of the fundamental dynamics of this photon-pair emission below.

Specifically, we prepare the system initially in the ground state, and the tunneling of a Cooper pair will draw energy quanta from the bias voltage, inducing the coherent transition $|0, 0, g\rangle \longrightarrow |1, 1, e\rangle$. Due to the energy upper limit of the two-level charge qubit, the system populated in the state $|1, 1, e\rangle$ can not be excited to higher energy levels. This indicates that a second Cooper pair can't pass through the circuit only after the spontaneously emission of the charge qubit. So, to guarantee the desired antibunching, it is crucial to meet the condition $\kappa \gg \gamma$, i.e., the coherence time of charge qubit is much longer than that of cavities. In this situation, the two cavities will take the lead to emit two correlated photons within the lifetime $1/\kappa$, stemming from the spontaneous emission of $|1, 1, e\rangle$ state via the photonic dissipation. Then, the wavefunction of the system is collapsed into the state $|0, 0, e\rangle$ but without Rabi flopping. Only after a quantum jump $|0, 0, e\rangle \longrightarrow |0, 0, g\rangle$ of the qubit state within a relative longer lifetime $1/\gamma$, a second Cooper pair can tunnel to restart the coherent transition $|0, 0, g\rangle \longrightarrow |1, 1, e\rangle$ for the next emission of a photon pair. This is the mechanism for generating antibunched photon pairs.

On the other hand, it is worth noting here that we also can not make an arbitrary small γ . For $\gamma \rightarrow 0$, the system seems to behave as a completely antibunched photon-pair source. However, it will take a very long time to flip the state of charge qubit $|0, 0, e\rangle \longrightarrow |0, 0, g\rangle$ and reconstruct the state $|1, 1, e\rangle$ for the two cavities to emit a next correlated photon pair. This will result in an extremely low emission rate.

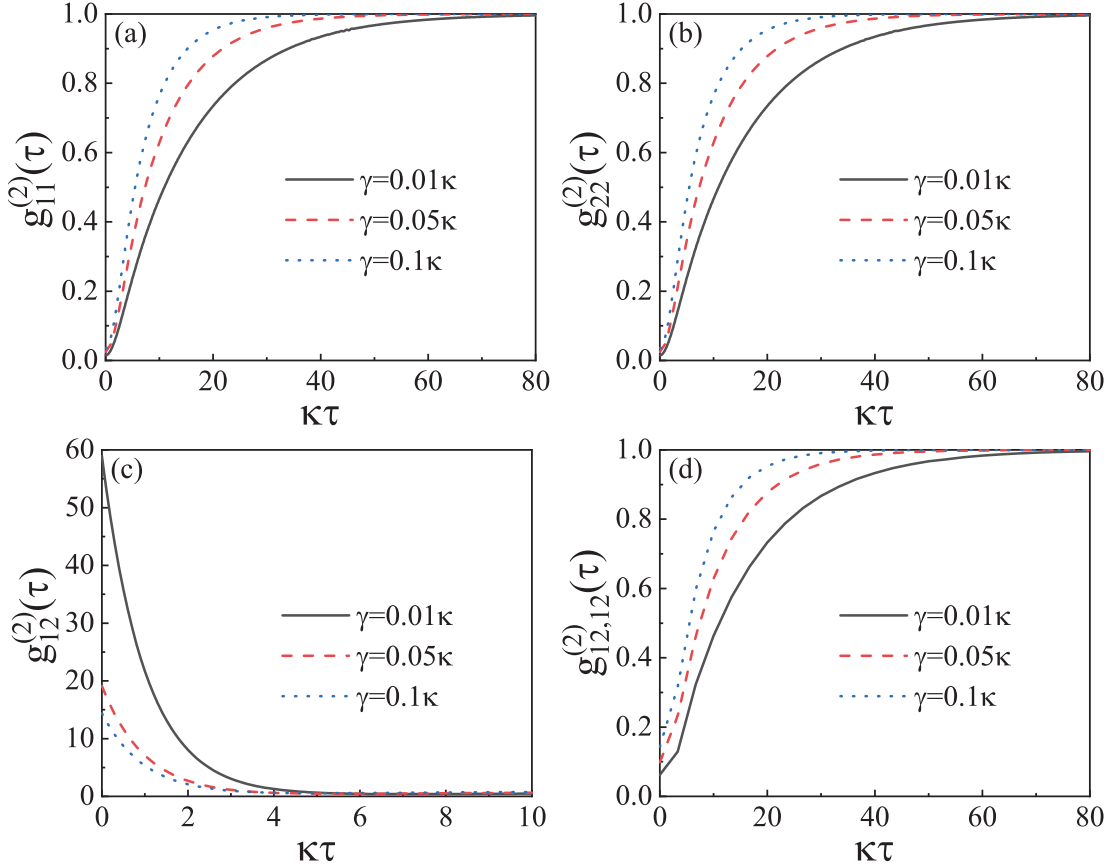


Figure 3. (Color online) Steady-state photon correlation functions versus $\kappa\tau$: [a], [b] for the stand second-order correlation functions $g_{11}^{(2)}(\tau)$, $g_{22}^{(2)}(\tau)$; [c] for the cross-correlation function $g_{12}^{(2)}(\tau)$; [d] for the generalized second-order correlation functions $g_{12,12}^{(2)}(\tau)$. The cavity damping rate is chosen as $\kappa/2\pi = 0.1$ GHz, and the other parameters are chosen to be the same as those in Figure 2.

Therefore, there is a tradeoff between the emission rate and the nonclassical property of the radiation field, which can be balanced by tuning the ratio γ/κ .

To describe the quantum statistics of the photon emission, we further study the following time-delay correlation functions

$$g_{pq}^{(2)}(\tau) = \frac{\langle a_p^\dagger(0)a_q^\dagger(\tau)a_q(\tau)a_p(0) \rangle}{\langle (a_p^\dagger a_p)(0) \rangle \langle (a_q^\dagger a_q)(\tau) \rangle} \quad (11)$$

with $p = 1, 2$ and $q = 1, 2$. For $p = q$, $g_{pq}^{(2)}(\tau)$ is just the standard second-order correlation function that can quantify the photon correlation emitted by a single cavity. While for $p \neq q$, it represents the cross-correlation between the photons emitted by different cavities. Besides, we should also introduce the generalized second-order correlation function

$$g_{12,12}^{(2)}(\tau) = \frac{\langle a_1^\dagger(0)a_2^\dagger(0)a_1^\dagger(\tau)a_2^\dagger(\tau)a_1(\tau)a_2(\tau)a_1(0)a_2(0) \rangle}{\langle (a_1^\dagger a_2^\dagger a_1 a_2)(0) \rangle \langle (a_1^\dagger a_2^\dagger a_1 a_2)(\tau) \rangle}, \quad (12)$$

where the joint two-photon emission event by the two cavities is considered as a single

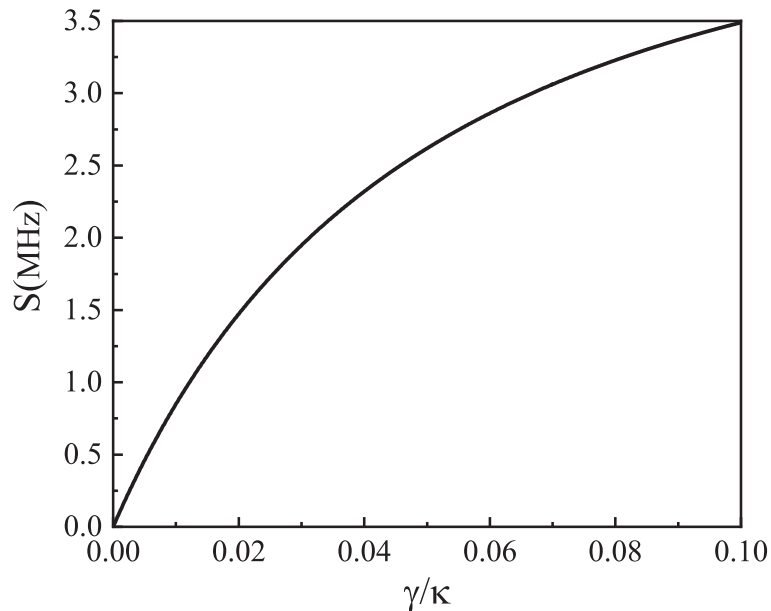


Figure 4. (Color online) The photon-pair emission rate S versus γ/κ . The relevant parameters are chosen to be the same as those in Figure 3.

entity [59, 60]. Here, $g_{12,12}^{(2)}(\tau)$ can capture the fundamental dynamics of photon-pair emission, and characterize the quantum statistics of photon pairs.

In Figure 3, we plot the different steady-state correlation functions by numerically solving the master equation (10). For $\kappa \gg \gamma$, the zero-delay second-order correlation functions $g_{11}^{(2)}(0) \rightarrow 0$ and $g_{22}^{(2)}(0) \rightarrow 0$ are observed in Figures 3(a) and 3(b), exhibiting distinct antibunching effects. So, each cavity behaves as an excellent single-photon emitter. As seen in Figure 3(c), the zero-delay cross-correlation function yields $g_{12}^{(2)}(0) \gg 1$. This indicates that a pair of strongly correlated photons are emitted simultaneously by the two cavities. Moreover, the generalized zero-delay second-order correlation function $g_{12,12}^{(2)}(0) \ll 1$ in Figure 3(d) manifests clearly that the two cavities release their energies in the form of antibunched photon pairs. In addition, as expected before, the changes of the different zero-delay correlation functions indicate that our device approaches a perfect photon-pair emitter with the decrease of γ .

Finally, we investigate the emission rate of our photon-pair source. It is defined as

$$S = \kappa \bar{n}, \quad (13)$$

where \bar{n} is the average photon numbers of the two cavities. The emission rate S versus γ/κ is displayed in Figure 4. Under the premise of $\kappa \gg \gamma$, we can observe that a tunable emission rate can be achieved, i.e., S gradually increases with the increase of γ . Hence, the emission rate can be experimentally controlled by changing the distance between the cavity and the transmission line to adjust the value of κ [35]. With the currently available parameters $\omega_1/2\pi = 9$ GHz, $\omega_2/2\pi = 7$ GHz, $\delta/2\pi = 5$ GHz, $E_J/2\pi = 0.5$ GHz, $\lambda_1 = \lambda_2 = 0.2$, we can obtain an emission rate of the order of MHz.

4. Conclusion

In conclusion, we have proposed a practical approach to generate antibunched photon pairs in a Josephson-photonics circuit of a dc voltage-biased Josephson junction coupled to both a superconducting charge qubit and two nondegenerate microwave cavities. Under an appropriate bias voltage, each Cooper pair can tunnel inelastically to cause the excitation of charge qubit and the creation of one photon in each cavity. We demonstrate that the charge transport can be controlled via the two-level charge qubit, preventing the simultaneous Cooper pair tunneling events. As a result, the photon-pair blockade can be realized, i.e., the presence of a qubit excitation will impede further photon absorption. Together with the photonic dissipation, the two cavities can emit antibunched pairs of two strongly correlated photons with a tunable emission rate. Moreover, the generation of such a nonclassical microwave source is compatible with current experimental architectures, and may stimulate a variety of applications in the field of quantum information science.

acknowledgments

This work was supported by the National Natural Science Foundation of China (Grant Nos. 11704306 and 12074307), the Fundamental Research Funds for the Central Universities (Grant No. 11913291000022), and the Doctoral Scientific Research Foundation of Hubei University of Automotive Technology (Grant No. BK202113).

Appendix A. Detailed derivation of equation (1) in the main text

As illustrated in Figure 1, the charge qubit is a mesoscopic superconducting island connected by a tunnel junction with capacitance C_q and Josephson coupling energy E_{Jq} [52–55]. A gate voltage V_g is coupled to the island to control the tunneling of Cooper pairs. Its Hamiltonian is given by

$$H_q = E_c(n_q - n_g)^2 - E_{Jq} \cos \phi_q, \quad (\text{A.1})$$

where $E_c = 2e^2/(C_q + C_g)$ denotes the charging energy of a Cooper pair, and $n_g = C_g V_g/2e$ is the dimensionless gate charge as a control parameter. n_q is the number of Cooper pairs on the island, and ϕ_q is the phase difference across the junction, which are conjugate variables that obey $[\phi_q, n_q] = i$.

The LC resonator consists of a capacitor C_j connected to an inductor L_j , and its Hamiltonian is written as

$$H_r = \sum_{j=1,2} \frac{q_j^2}{2C_j} + \left(\frac{\hbar}{2e}\right)^2 \frac{\phi_j^2}{2L_j}, \quad (\text{A.2})$$

where q_j and ϕ_j represent the charge and phase operators acting on the capacitor C_j and the inductor L_j , respectively. They form a canonical conjugate pair, and satisfy the commutation relation $[\phi_j, q_j] = 2ei$.

The dc-SQUID is made up of two identical Josephson junctions and can be treated as a tunable Josephson junction with effective Josephson energy $E_J = 2E_{J0} \cos(\pi\Phi_{\text{ext}}/\Phi_0)$, which can be tuned by controlling the magnetic flux Φ_{ext} penetrating its loop area [46]. Here E_{J0} is the Josephson junction energy of a single junction, and $\Phi_0 = h/2e$ is the magnetic flux quantum. The Hamiltonian of the SQUID takes the form

$$H_J = -E_J \cos \phi_J - 2en_J V_J, \quad (\text{A.3})$$

where ϕ_J is the phase difference across the SQUID, and n_J counts the number of Cooper pairs that have transferred the junctions. These two variables obey the commutation relation $[\phi_J, n_J] = i$. Additionally, $V_J = -\hbar\dot{\phi}_J/2e$ represents the voltage drop across the SQUID. In the presence of the bias voltage V , we have $V_J = V - V_q - V_{R1} - V_{R2}$ according to Kirchhoff's rules, where $V_q = -\hbar\dot{\phi}_q/2e$ is the voltage drop at the qubit, and $V_{Rj} = -\hbar\dot{\phi}_j/2e$ is the voltage drop at the j -th resonator. By replacing V_J with $V - V_q - V_{R1} - V_{R2}$ in equation (A.3), we have

$$H_J = -E_J \cos \phi_J - 2en_J(V - V_q - V_{R1} - V_{R2}). \quad (\text{A.4})$$

Together with the equations (A.1), (A.2) and (A.4), we can give the total Hamiltonian of the whole system

$$H_T = H_q + H_r + H_J, \quad (\text{A.5})$$

which is just the equation (1) in the main text.

References

- [1] Blais A, Grimsmo A L, Girvin S M and Wallraff A 2021 *Rev. Mod. Phys.* **93**(2) 025005 URL <https://link.aps.org/doi/10.1103/RevModPhys.93.025005>
- [2] Arute F, Arya K, Babbush R, Bacon D, Bardin J C, Barends R, Biswas R, Boixo S, Brandao F G S L, Buell D A, Burkett B, Chen Y, Chen Z, Chiaro B, Collins R, Courtney W, Dunsworth A, Farhi E, Foxen B, Fowler A, Gidney C, Giustina M, Graff R, Guerin K, Habegger S, Harrigan M P, Hartmann M J, Ho A, Hoffmann M, Huang T, Humble T S, Isakov S V, Jeffrey E, Jiang Z, Kafri D, Kechedzhi K, Kelly J, Klimov P V, Knysh S, Korotkov A, Kostritsa F, Landhuis D, Lindmark M, Lucero E, Lyakh D, Mandrà S, McClean J R, McEwen M, Megrant A, Mi X, Michielsen K, Mohseni M, Mutus J, Naaman O, Neeley M, Neill C, Niu M Y, Ostby E, Petukhov A, Platt J C, Quintana C, Rieffel E G, Roushan P, Rubin N C, Sank D, Satzinger K J, Smelyanskiy V, Sung K J, Trevithick M D, Vainsencher A, Villalonga B, White T, Yao Z J, Yeh P, Zalcman A, Neven H and Martinis J M 2019 *Nature* **574** 505–510
- [3] Wu Y, Bao W S, Cao S, Chen F, Chen M C, Chen X, Chung T H, Deng H, Du Y, Fan D, Gong M, Guo C, Guo C, Guo S, Han L, Hong L, Huang H L, Huo Y H, Li L, Li N, Li S, Li Y, Liang F, Lin C, Lin J, Qian H, Qiao D, Rong H, Su H, Sun L, Wang L, Wang S, Wu D, Xu Y, Yan K, Yang W, Yang Y, Ye Y, Yin J, Ying C, Yu J, Zha C, Zhang C, Zhang H, Zhang K, Zhang Y, Zhao H, Zhao Y, Zhou L, Zhu Q, Lu C Y, Peng C Z, Zhu X and Pan J W 2021 *Phys. Rev. Lett.* **127**(18) 180501 URL <https://link.aps.org/doi/10.1103/PhysRevLett.127.180501>
- [4] Gu X, Kockum A F, Miranowicz A, xi Liu Y and Nori F 2017 **718-719** 1–102
- [5] Hofheinz M, Weig E M, Ansmann M, Bialczak R C, Lucero E, Neeley M, O'Connell A D, Wang H, Martinis J M and Cleland A N 2008 *Nature* **454** 310–314
- [6] Ofek N, Petrenko A, Heeres R, Reinhold P, Leghtas Z, Vlastakis B, Liu Y, Frunzio L, Girvin S M, Jiang L, Mirrahimi M, Devoret M H and Schoelkopf R J 2016 *Nature* **536** 441–445

- [7] Hofheinz M, Portier F, Baudouin Q, Joyez P, Vion D, Bertet P, Roche P and Esteve D 2011 *Phys. Rev. Lett.* **106**(21) 217005 URL <https://link.aps.org/doi/10.1103/PhysRevLett.106.217005>
- [8] Padurariu C, Hassler F and Nazarov Y V 2012 *Phys. Rev. B* **86**(5) 054514 URL <https://link.aps.org/doi/10.1103/PhysRevB.86.054514>
- [9] Koppenhöfer M, Leppäkangas J and Marthaler M 2017 *Phys. Rev. B* **95**(13) 134515 URL <https://link.aps.org/doi/10.1103/PhysRevB.95.134515>
- [10] Leppäkangas J, Johansson G, Marthaler M and Fogelström M 2013 *Phys. Rev. Lett.* **110**(26) 267004 URL <https://link.aps.org/doi/10.1103/PhysRevLett.110.267004>
- [11] Forgues J C, Lupien C and Reulet B 2014 *Phys. Rev. Lett.* **113**(4) 043602 URL <https://link.aps.org/doi/10.1103/PhysRevLett.113.043602>
- [12] Forgues J C, Lupien C and Reulet B 2015 *Phys. Rev. Lett.* **114**(13) 130403 URL <https://link.aps.org/doi/10.1103/PhysRevLett.114.130403>
- [13] Danner L, Padurariu C, Ankerhold J and Kubala B 2021 *Phys. Rev. B* **104**(5) 054517 URL <https://link.aps.org/doi/10.1103/PhysRevB.104.054517>
- [14] Mora C, Altimiras C, Joyez P and Portier F 2017 *Phys. Rev. B* **95**(12) 125311 URL <https://link.aps.org/doi/10.1103/PhysRevB.95.125311>
- [15] Leppäkangas J, Fogelström M, Marthaler M and Johansson G 2016 *Phys. Rev. B* **93**(1) 014506 URL <https://link.aps.org/doi/10.1103/PhysRevB.93.014506>
- [16] Saira O P, Zgirski M, Viisanen K L, Golubev D S and Pekola J P 2016 *Phys. Rev. Applied* **6**(2) 024005 URL <https://link.aps.org/doi/10.1103/PhysRevApplied.6.024005>
- [17] Meister S, Mecklenburg M, Gramich V, Stockburger J T, Ankerhold J and Kubala B 2015 *Phys. Rev. B* **92**(17) 174532 URL <https://link.aps.org/doi/10.1103/PhysRevB.92.174532>
- [18] Armour A D, Kubala B and Ankerhold J 2015 *Phys. Rev. B* **91**(18) 184508 URL <https://link.aps.org/doi/10.1103/PhysRevB.91.184508>
- [19] Armour A D, Kubala B and Ankerhold J 2017 *Phys. Rev. B* **96**(21) 214509 URL <https://link.aps.org/doi/10.1103/PhysRevB.96.214509>
- [20] Wang H, Blencowe M P, Armour A D and Rimberg A J 2017 *Phys. Rev. B* **96**(10) 104503 URL <https://link.aps.org/doi/10.1103/PhysRevB.96.104503>
- [21] Kubala B, Ankerhold J and Armour A D 2020 *New J. Phys.* **22** 023010
- [22] Armour A D, Blencowe M P, Brahim E and Rimberg A J 2013 *Phys. Rev. Lett.* **111**(24) 247001 URL <https://link.aps.org/doi/10.1103/PhysRevLett.111.247001>
- [23] Gramich V, Kubala B, Rohrer S and Ankerhold J 2013 *Phys. Rev. Lett.* **111**(24) 247002 URL <https://link.aps.org/doi/10.1103/PhysRevLett.111.247002>
- [24] Dambach S, Kubala B, Gramich V and Ankerhold J 2015 *Phys. Rev. B* **92**(5) 054508 URL <https://link.aps.org/doi/10.1103/PhysRevB.92.054508>
- [25] Souquet J R and Clerk A A 2016 *Phys. Rev. A* **93**(6) 060301 URL <https://link.aps.org/doi/10.1103/PhysRevA.93.060301>
- [26] Leppäkangas J and Marthaler M 2018 *Phys. Rev. B* **98**(22) 224511 URL <https://link.aps.org/doi/10.1103/PhysRevB.98.224511>
- [27] Marthaler M, Leppäkangas J and Cole J H 2011 *Phys. Rev. B* **83**(18) 180505 URL <https://link.aps.org/doi/10.1103/PhysRevB.83.180505>
- [28] Morley W T, Di Marco A, Mantovani M, Stadler P, Belzig W, Rastelli G and Armour A D 2019 *Phys. Rev. B* **100**(5) 054515 URL <https://link.aps.org/doi/10.1103/PhysRevB.100.054515>
- [29] Dambach S, Armour A D, Kubala B and Ankerhold J 2019 *Phys. Scr.* **94** 104001
- [30] Chen F, Li J, Armour A D, Brahim E, Stettenheim J, Sirois A J, Simmonds R W, Blencowe M P and Rimberg A J 2014 *Phys. Rev. B* **90**(2) 020506 URL <https://link.aps.org/doi/10.1103/PhysRevB.90.020506>
- [31] Cassidy M C, Bruno A, Rubbert S, Irfan M, Kammhuber J, Schouten R N, Akhmerov A R and Kouwenhoven L P 2017 *Science* **355** 939–942

- [32] Simon S H and Cooper N R 2018 *Phys. Rev. Lett.* **121**(2) 027004 URL <https://link.aps.org/doi/10.1103/PhysRevLett.121.027004>
- [33] Kubala B, Gramich V and Ankerhold J 2015 *Phys. Scr.* **T165** 014029
- [34] Leppäkangas J, Fogelström M, Grimm A, Hofheinz M, Marthaler M and Johansson G 2015 *Phys. Rev. Lett.* **115**(2) 027004 URL <https://link.aps.org/doi/10.1103/PhysRevLett.115.027004>
- [35] Rolland C, Peugeot A, Dambach S, Westig M, Kubala B, Mukharsky Y, Altimiras C, le Sueur H, Joyez P, Vion D, Roche P, Esteve D, Ankerhold J and Portier F 2019 *Phys. Rev. Lett.* **122**(18) 186804 URL <https://link.aps.org/doi/10.1103/PhysRevLett.122.186804>
- [36] Grimm A, Blanchet F, Albert R, Leppäkangas J, Jebari S, Hazra D, Gustavo F, Thomassin J L, Dupont-Ferrier E, Portier F and Hofheinz M 2019 *Phys. Rev. X* **9**(2) 021016 URL <https://link.aps.org/doi/10.1103/PhysRevX.9.021016>
- [37] Lang B and Armour A D 2021 *New J. Phys.* **23** 033021
- [38] Ma S l, Li X k, Ren Y l, Xie J k and Li F l 2021 *Phys. Rev. Research* **3**(4) 043020 URL <https://link.aps.org/doi/10.1103/PhysRevResearch.3.043020>
- [39] Ménard G C, Peugeot A, Padurariu C, Rolland C, Kubala B, Mukharsky Y, Iftikhar Z, Altimiras C, Roche P, le Sueur H, Joyez P, Vion D, Esteve D, Ankerhold J and Portier F 2021 *arXiv:2111.09604* URL <https://arxiv.org/abs/2111.09604>
- [40] Jebari S, Blanchet F, Grimm A, Hazra D, Albert R, Joyez P, Vion D, Estève D, Portier F and Hofheinz M 2018 *Nat. Electronics.* **1** 223–227
- [41] Dambach S, Kubala B and Ankerhold J 2017 *New J. Phys.* **19** 023027
- [42] Leppäkangas J, Marthaler M, Hazra D, Jebari S, Albert R, Blanchet F, Johansson G and Hofheinz M 2018 *Phys. Rev. A* **97**(1) 013855 URL <https://link.aps.org/doi/10.1103/PhysRevA.97.013855>
- [43] Armour A D, Kubala B and Ankerhold J 2015 *Phys. Rev. B* **91**(18) 184508 URL <https://link.aps.org/doi/10.1103/PhysRevB.91.184508>
- [44] Trif M and Simon P 2015 *Phys. Rev. B* **92**(1) 014503 URL <https://link.aps.org/doi/10.1103/PhysRevB.92.014503>
- [45] Arndt L and Hassler F 2019 *Phys. Rev. B* **100**(1) 014505 URL <https://link.aps.org/doi/10.1103/PhysRevB.100.014505>
- [46] Westig M, Kubala B, Parlavecchio O, Mukharsky Y, Altimiras C, Joyez P, Vion D, Roche P, Esteve D, Hofheinz M, Trif M, Simon P, Ankerhold J and Portier F 2017 *Phys. Rev. Lett.* **119**(13) 137001 URL <https://link.aps.org/doi/10.1103/PhysRevLett.119.137001>
- [47] Westig M, Kubala B, Parlavecchio O, Mukharsky Y, Altimiras C, Joyez P, Vion D, Roche P, Esteve D, Hofheinz M, Trif M, Simon P, Ankerhold J and Portier F 2017 *Phys. Rev. Lett.* **119**(13) 137001 URL <https://link.aps.org/doi/10.1103/PhysRevLett.119.137001>
- [48] Pan J W, Chen Z B, Lu C Y, Weinfurter H, Zeilinger A and Żukowski M 2012 *Rev. Mod. Phys.* **84**(2) 777–838 URL <https://link.aps.org/doi/10.1103/RevModPhys.84.777>
- [49] Benson O, Santori C, Pelton M and Yamamoto Y 2000 *Phys. Rev. Lett.* **84**(11) 2513–2516 URL <https://link.aps.org/doi/10.1103/PhysRevLett.84.2513>
- [50] Jayakumar H, Predojević A, Huber T, Kauten T, Solomon G S and Weihs G 2013 *Phys. Rev. Lett.* **110**(13) 135505 URL <https://link.aps.org/doi/10.1103/PhysRevLett.110.135505>
- [51] Huber D, Reindl M, Covre da Silva S F, Schimpf C, Martín-Sánchez J, Huang H, Piredda G, Edlinger J, Rastelli A and Trotta R 2018 *Phys. Rev. Lett.* **121**(3) 033902 URL <https://link.aps.org/doi/10.1103/PhysRevLett.121.033902>
- [52] Bouchiat V, Vion D, Joyez P, Esteve D and Devoret M H 1998 *Phys. Scr.* **T76** 165
- [53] Makhlin Y, Scöhn G and Shnirman A 1999 *Nature* **398** 305–307
- [54] Nakamura Y, Pashkin Y A and Tsai J S 1999 *Nature* **398** 786–788
- [55] Blais A, Huang R S, Wallraff A, Girvin S M and Schoelkopf R J 2004 *Phys. Rev. A* **69**(6) 062320 URL <https://link.aps.org/doi/10.1103/PhysRevA.69.062320>
- [56] Cahill K E and Glauber R J 1969 *Phys. Rev.* **177**(5) 1857–1881 URL

- <https://link.aps.org/doi/10.1103/PhysRev.177.1857>
- [57] Hamsen C, Tolazzi K N, Wilk T and Rempe G 2017 *Phys. Rev. Lett.* **118**(13) 133604 URL <https://link.aps.org/doi/10.1103/PhysRevLett.118.133604>
- [58] Felicetti S, Rossatto D Z, Rico E, Solano E and Forn-Díaz P 2018 *Phys. Rev. A* **97**(1) 013851 URL <https://link.aps.org/doi/10.1103/PhysRevA.97.013851>
- [59] Muñoz C S, del Valle E, Tudela A G, Müller K, Lichtmannecker S, Kaniber M, Tejedor C, Finley J J and Laussy F P 2014 *Nat. Photonics* **8** 550–555
- [60] Ren Y, Duan S, Xie W, Shao Y and Duan Z 2021 *Phys. Rev. A* **103**(5) 053710 URL <https://link.aps.org/doi/10.1103/PhysRevA.103.053710>